 doi:10.20944/preprints201912.0238.v1

Title:

Ccr6 deficiency attenuates spontaneous chronic colitis in Winnie.

First Author: **Ranmali Ranasinghe**[1] hewausaramba.ranasinghe@UTAS.EDU.AU ORCID

Other Authors: Ruchira Fernando[2], Promoda Perera[1], Madhur Shastri[1], Waheedha Basheer[1], Paul Scowen[3], Terry Pinfold[3] and Rajaraman Eri[1].

Affiliations:

1 School of Health Sciences, College of Health and Medicine, University of Tasmania, Launceston 7250, Tasmania, Australia.

2 Department of Histopathology, Launceston General Hospital, Launceston 7250, Tasmania, Australia.

3 School of Medicine, University of Tasmania, Hobart 7000, Tasmania, Australia.

Author for communication: Rajaraman Eri, rderi@utas.edu.au

ABSTRACT

The immunomodulatory behaviour of the CCR6/CCL20 axis on multi -system pathophysiology and molecular signalling was investigated at two clinically significant time points, using a *Ccr6* - deficient mouse model of spontaneous colitis. Four groups of mice, (C57BL/6J, *Ccr6*-/- of C57BL/6J, Winnie x *Ccr6* -/- and Winnie) were utilized and (I) colonic clinical parameters (2) histology of colon, spleen, kidney and liver (3) T and B lymphocyte distribution in the spleen and MLN by flowcytometry (5) colonic CCL20, PI3K and phosphorylated Akt expression by immunohistochemistry and (6) colonic cytokine expression by RT-PCR were evaluated. CCR6 influenced upregulation of inflammation in the spleen, liver and gut while renal histology remained unaffected. Marked focal lobular inflammation with reactive nuclear features were observed in hepatocytes and a significant neutrophil infiltration in red pulp with extra medullary hemopoiesis in the spleen existed in Winnie. These changes were considerably reduced in Winnie x *Ccr6*-/- with elevated goblet cell numbers and mucus production in the colonic epithelium. Results indicate that *Ccr6*- deficiency in the colitis model contributes towards resolution of disease. Our findings demonstrate an intricate networking role for CCR6 in immune activation, which is downregulated by *Ccr6* deficiency, and could provide newer clinical therapies in colitis.

Preprints (www.preprints.org) | NOT PEER-REVIEWED | Posted: 18 December 2019 doi:10.20944/preprints201912.0238.v1

1.0 Introduction

A plethora of therapies have been tried to date in the treatment of inflammatory bowel disease (IBD) except for CC -chemokine receptor 6 (CCR6) -inhibition (1). This study aims at elucidating the effects of CCR6 - deficiency in an inflammatory setting of chronic spontaneous colitis. Winnie, a time-tested and proven model of murine spontaneous colitis which closely resembles human ulcerative colitis (UC) was used in which the *Ccr6* gene was knocked out (2). We determined some clinical, histological and immunological parameters which delineates the impact of CCR6 - deficiency in terms of its potentiality to become a proactive drug target. Additionally, we have investigated the sequel of CCR6 - deficiency in multi-system pathophysiology with the spleen, liver and kidneys to identify a link between the gut and other organs in the spread of microbial dysbiosis which commonly stems within the enteric system (3). These findings are expected to open avenues to a more detailed examination of CCR6 immunobiology and physiology to evaluate the impact of CCR6 - inhibition as a modernistic treatment option in IBD.

IBD is a globalised immune compromised disease complex having two concordant phenotypes; Crohn's disease (CD) and Ulcerative colitis (UC) in the human gut that are characterized by chronic intestinal inflammation (4). IBD causes severe morbidity in young adults who are at the educationally and economically most productive age (5). The disease itself places a heavy burden on the patients by causing psychological distress such as annihilating career objectives, instilling social stigma and deteriorating their quality of life (6). It produces a series of relapses and remissions with colectomy as the final treatment option and a high risk of developing colorectal cancer (CRC) (7).

The anticipated benefits that justify our study are the existing compelling evidence that CCR6 has multiple immune functions in many organ systems of humans and is considered a valuable therapeutic target (8). From preclinical studies, it is hoped that the immune cell triggers or pathways that arise from CCR6 activation could be identified (9). These results could then be translated into clinical trials which target the neutralization of CCR6 or its associated cytokines/ products /mediators in human colitis. Sixteen tractable inhibitors of CCR6 and its sole ligand, CC-motif chemokine ligand 20 (CCL20) have already been identified and some have even undergone clinical trials for the treatment of several autoimmune disorders such as experimental autoimmune encephalitis (EAE), rheumatoid arthritis (RA) and psoriasis (1). No such clinical trials have been performed with the existing inhibitors up to date in IBD, which is also considered by some as an autoimmune disease (1).

Chemokines are small protein molecules which act as chemoattractant cytokines and consist of two cohorts, the receptors and ligands (10). The receptors are present on a wide range of immune and non-immune cell types. CCL20 is produced in copious amounts by the gut epithelium in response to infectious microbial penetration which attracts the immune cells bearing CCR6 to the site of infection (10). CCR6-CCL20 axis fundamentally aids leukocyte homeostasis in the intestines and this CCR6-deficient mouse model is used to understand how the immune mechanisms work towards restoring immune cell balance in the steady state as seen in a healthy person (11).

Ccr6 is the gene which encodes for the CCR6 receptor and mice expressing spontaneous colitis in which this gene was deleted have displayed increased resistance to inflammation simply limiting it to the proximal colonic segment and having an inflammation-free mid to distal colon (11). This was first written in the doctoral thesis of W. Basheer (2018) which has been further validated by this study (11). Phenotypical assessment of colonic inflammatory markers, histological parameters and immunological evaluation have placed our

Preprints (www.preprints.org) | NOT PEER-REVIEWED | Posted: 18 December 2019 doi:10.20944/preprints201912.0238.v1

model under investigation, Winnie X *Ccr6*-/-, in an intermediate rank compared to the healthy WT and the acutely diseased Winnie. Winnie mice display immune responses by a threefold increase of immune cells in the colon compared to WT mice with a significant increase in mucosal cytokine secretion in the gut and produce disease like that of human UC (12). By crossing Winnie mice with WT deficient in *Ccr6*, we have induced a mild, chronic colitis, strongly resembling human UC in our Winnie X *Ccr6*-/-, which is homozygous for two gene deficiencies, *Muc2* and *Ccr6*. Chronic colitis in Winnie is caused by a primary epithelial cell defect activated by a point mutation in the *Muc2* gene resulting in aberrant mucin-2 biosynthesis (2). It leads to endoplasmic reticulum stress in intestinal goblet cells and reduced secretion of mucus (13). Winnie mice display symptoms of diarrhoea, ulcerations, rectal bleeding and pain at different stages of colitis synonymous with human disease. Exhaustive studies done in Winnie have proven it to be the best available murine model to study human chronic colitis and its pathogenesis (12). Therefore, this study has become highly clinically relevant in most of its aspects.

4 groups of mice (C57BL/6J, *Ccr6* KO of C57BL/6J, Winnie X *Ccr6*-/- and Winnie) were tested at 8 weeks and between 16-20 weeks of age (Table 1). Chronic gut inflammation is known to take a hold by 6 weeks of age in Winnie and manifests into acute colitis by 16 weeks of age (2). Inflammation was evaluated in the colon beginning from the ileo-caecal junction to the anus using commonly used inflammatory parameters and histological schemata (14). Considering the pleiotropic immune functions displayed by CCR6 in multiple organs in the human body, which have influenced the immunogenic outcome of many clinical diseases associated with the said organs, this study also made a histological assessment of the spleen, liver and kidneys at the two given time points, after a morphological examination and recording the weight. A detailed histological and immunohistochemical study was carried out to evaluate inflammation in the colon paying special attention to the expression patterns of the chemokine CCL20, PI3K and phosphorylated Akt as well as the quantification of both inflammatory and anti-inflammatory cytokine mRNA expression in the colon biopsies to elucidate a direct relationship between the CCR6-CCL20 leading to other immune pathways. The aim of this study was to investigate the therapeutic potential of CCR6 in Winnie X *Ccr6*-/- and our results show a considerable reduction in colitis.

2.0 Materials and Methods

2.1 Animals

All mice experiments were conducted under the Ethics permit number A17451 of the Animal Ethics Committee of the University of Tasmania in accordance with the Australian Code of Practice for Care and Use of Animals for Scientific Purposes (8th Edition 2013). Mice were housed in a temperature-controlled PC2 animal facility with a 12-hour day/night light cycle. Individual body weights were maintained daily over an initial acclimation period of 7 days. All mice were given radiation-sterilised rodent feed and autoclaved tap water for drinking ad libitum during experiments. All efforts were made to minimize animals' suffering and to reduce the number of animals used. Mice utilised were in the age group of 8 – 20 weeks.

Preprints (www.preprints.org) | NOT PEER-REVIEWED | Posted: 18 December 2019 doi:10.20944/preprints201912.0238.v1

Animal Strain	Age	Sex	Phenotype	Number	Description
C57BL/6J	8-20 weeks	M/F	Wild type	15	Healthy Control
Ccr6-/-	8-20 weeks	M/F	Targeted knockout	12	Negative Control
Winnie X *Ccr6-/-*	8-20 weeks	M/F	Targeted knockout	12	Study Model
Winnie	8-20 weeks	M/F	Muc2 mutation	12	Positive Control

Table 1: Experimental Strains of mice utilised with a description of age, sex, phenotype, numbers culled and their role in the research project. The mice were utilised in 2 batches, at 8 weeks and 16-20 weeks for separate clinical assessment.

2.2 Phenotypic Assessment

The phenotype was assessed using clinical parameters of each group of mice. The body weight was recorded prior to culling. The mice were culled using carbon dioxide euthanasia and were dissected under sterile conditions. The large intestine was separated at the ileo-caecal junction and the anus and placed on a non-absorbent surface. The length of the colon was measured from the Caeco-colic junction to the anus and was recorded. The whole colon was cut open along the longitudinal axis, faecal matter removed, and weight was recorded.

2.3 Morphological Assessment of other Organs

The spleen, kidneys and liver were harvested and weight of each was recorded. Both the kidneys were weighed together and general morphology such as size, colour, shape and texture were observed.

2.4 Flowcytometry

Mouse spleen was stored in ice-cold phosphate buffered saline (PBS; pH 7.4- Dulbecco's, 10 x L, Gibco, Life Technologies Pty Ltd, Victoria, Australia) on ice after which it was processed for analysis by flowcytometry. Mesenteric lymph nodes were harvested and stored in ice-cold RPMI 1640 culture medium (Life Technologies Pty Ltd, Victoria, Australia). Spleen and mesenteric lymph nodes were macerated using the end of a syringe plunger with ice-cold PBS and passed through a 70 µ corning cell strainer (Catalogue No. 08-771-2, Thermofisher Scientific Pty Ltd, Victoria, Australia) to prepare a homogenous suspension which was centrifuged at 500g for 10 minutes at 4°C (Allegra X15R Beckman Coulter, USA) to obtain a cell pellet. The RBC were removed by adding RBC lysis buffer (Catalogue No. 420301, Australian Biosearch Pty Ltd, Wangarra, WA, Australia). Ice-cold PBS was added to inactivate the RBC lysis buffer and centrifuged at 500g for 7 minutes at 4°C. FACS buffer was added to the RBC-free splenocyte samples and kept on ice. The number of cells were enumerated using trypan blue and 2 X 10^7 cells per mL was adjusted by adding FACS buffer. Sample was centrifuged at 500g for 7 minutes in a microcentrifuge to obtain a cell pellet. The supernatant was discarded, and fluorescent conjugated antibody (CD4- BV421, CD8a- AF488, CD19-PE) was added and vortexed briefly to mix and incubated on ice in the dark for 30 minutes. The cells were washed in PBS at 500g for 7 minutes, suspended in FACS buffer and flow cytometric data was obtained using a BD FACS CANTO™ flow cytometer (BD Biosciences, USA) and analysed using FCS Express version 6.06.0014 (De Novo Software, USA) for windows. Mesenteric lymph node suspensions were processed the same way except for the addition of RBC lysis buffer.

Preprints (www.preprints.org) | NOT PEER-REVIEWED | Posted: 18 December 2019 doi:10.20944/preprints201912.0238.v1

2.5 Histology

One half of the colon cut length wise was rolled into a swiss roll, liver, spleen and kidney and preserved in 10% neutral buffered formalin and transferred into 70% ethanol after 3-4 days. After chemical processing, were embedded in paraffin and sections cut to a thickness of 30 microns by a rotary microtome and were stained with Gill's haematoxylin and eosin (H&E). The H&E stained sections were imaged using an Olympus DP72 microscope. The tissue sections from all animals were scored in a blinded manner after grading for colitis by the histopathologist involved in this study at the Launceston General Hospital. Cell counting was performed manually in 10 random microscopic fields at magnifications of x400.

2.6 Immunohistochemistry

Paraffin-embedded colon tissue sections were dewaxed, processed in xylene and rehydrated in a series of ethanol. Antigen retrieval was carried out, hydrogen peroxide incubation was performed followed by the protein blocking using the Rabbit specific HRP/DAB (ABC) detection IHC kit (Catalogue No. 64261, Abcam, UK) following the manufacturer's protocol. Slides were washed under running water and rinsed in PBS (Dulbecco's, Invitrogen, Australia) after each treatment. Primary antibody diluted 1:500 was added and incubated for 1 hour in the dark inside a humidified chamber at room temperature (RT) followed by secondary antibody for 30 minutes. DAB chromogen + substrate buffer (1 drop of DAB chromogen diluted in 1 mL substrate buffer) was added to the tissue sections for 10 minutes and washed in PBS and counterstained with strong liquid Mayer's haematoxylin for 30 seconds, dipped in ammonia water and dehydrated in ethanol and xylene, cover slipped after adding a mounting medium. Percentage expression of intensity was calculated by the formula; optical density (OD) = log (maximum intensity/mean intensity), where max intensity = 255 for 8-bit images using Fiji Image J Version 1.64 software for windows 7 (Scijava Software Inc, USA).

2.7 Alcian Blue staining of mucus producing goblet cells

Deparaffinize slides and rehydrate in a series of alcohol. Stain with Alcian blue pH 2.5 for 30 minutes, wash in running water for 2 minutes, rinse in distilled water, counterstain with 0.1% nuclear fast red for 5 minutes, wash and dehydrate in alcohol, clear in xylene and mount. Acid mucins stain blue and nuclei stain in pink.

2.8 Statistical Data analysis

The data was analysed using Graph Pad Prism version 5.01 (Graph Pad Software Inc., USA). All data were expressed as mean $\pm$ standard error of the mean (SEM). The data were evaluated with One-way analysis of variance (ANOVA) and comparisons between groups were analysed using Tukey's multiple comparison tests. The data were considered significant when $p \leq 0.05$ (*), $p \leq 0.01$ (**), $p \leq 0.001$ (***) and $p \leq 0.0001$ (****).

3.0 Results

3.1 Clinical Parameters

3.1.1 Colon Length

As part of investigating the clinical parameters, the colon length of the four genotypes was measured in freshly removed colons from the ileocecal junction to anus using a ruler. WT remained in similar proportions to all four genotypes at 8 weeks of age (WT: 8.4 $\pm$ 0.14 cm, *Ccr6*-/-: 8.4 $\pm$ 0.25 cm, Winnie x *Ccr6*-/-: 8.2 $\pm$ 0.25 cm, Winnie: 8.6 $\pm$ 0.27 cm). At 16-20 weeks

Preprints (www.preprints.org) | NOT PEER-REVIEWED | Posted: 18 December 2019 doi:10.20944/preprints201912.0238.v1

(WT: 8.0 ± 0.33 cm, *Ccr6*-/-: 8.5 ± 0.6 cm, Winnie x *Ccr6*-/-: 9.0 ± 0.46 cm, Winnie: 10 ± 0.74 cm) among the four genotypes, the colon length was longest in Winnie and the colon length was shortest in the WT. A significant difference in colon length exists at the 16-20 weeks- time point between WT and Winnie (***p<0.001) as well as WT and Winnie x *Ccr6*-/- (**p ≤ 0.01).

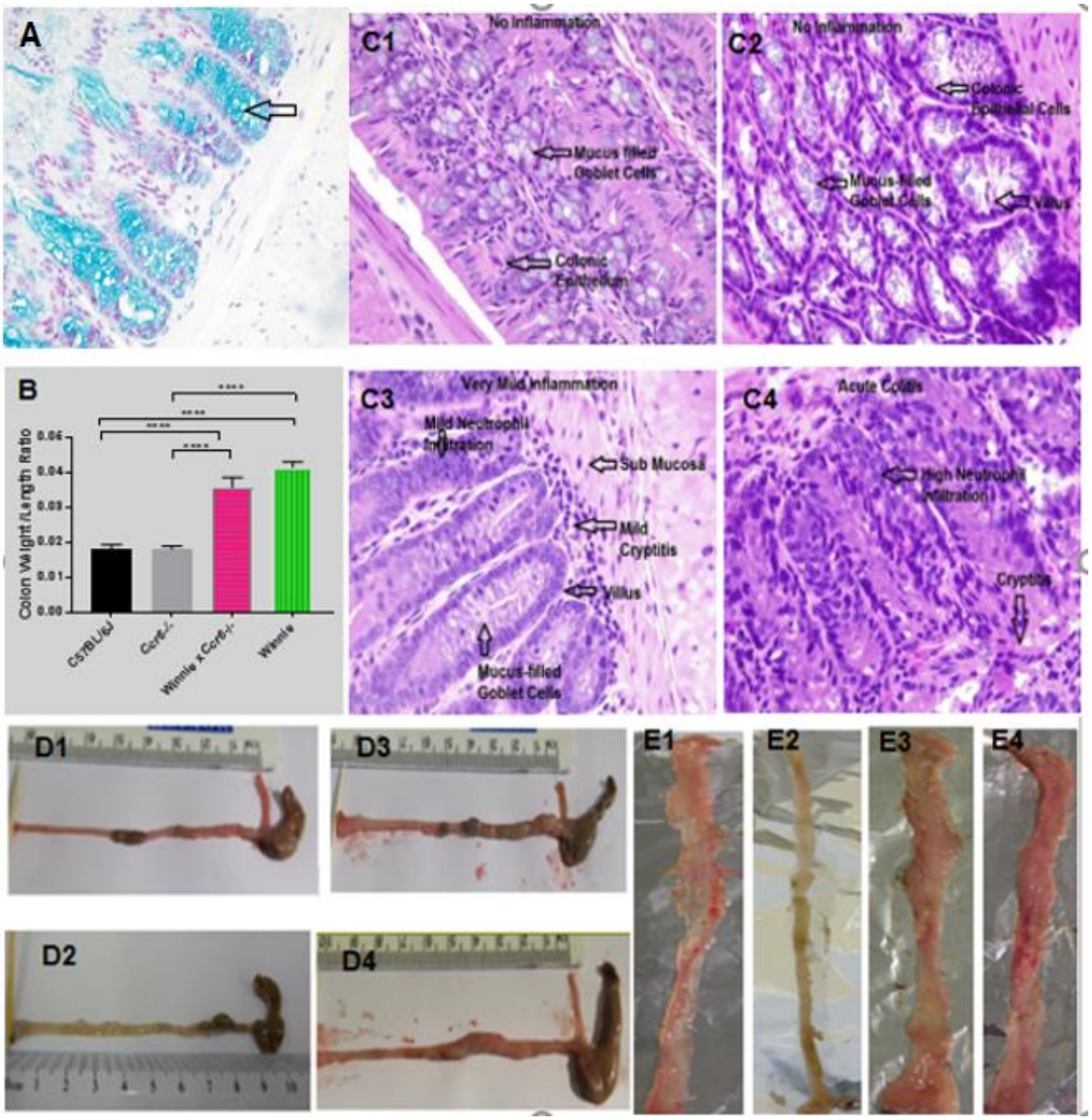

Figure 1: Comparison of the clinical parameters of freshly removed colons measured from the ileo-caecal junction to the anus in the four genotypes at 16-20 weeks. Data expressed as mean ± SEM by repeated measures analysis of variance (ANOVA) and Tukey's multiple comparison test, n=8 per group. (A) arrow indicating alcian blue test to confirm presence of mucin in colonic epithelial cells in Winnie x *Ccr6*-/- (B) colon weight/ body weight ratio at 16-20 weeks of age (C) colon histology (D) gross colon morphology before sectioning and (E) colon morphology after longitudinal sectioning and removal of luminal contents; 1- WT, 2- *Ccr6-/-,* 3- Winnie x *Ccr6-/-,* 4-Winnie. p ≤ 0.01 (**), p ≤ 0.001 (***) and p ≤ 0.0001 (****).

Preprints (www.preprints.org) | NOT PEER-REVIEWED | Posted: 18 December 2019 doi:10.20944/preprints201912.0238.v1

3.1.2 Colon Weight

The wet colon weight was measured using freshly removed colons, after removing the luminal contents. At 8 weeks, (WT: 0.1 ± 0.02 g, *Ccr6*-/-: 0.15 ± 0.02 g, Winnie x *Ccr6*-/-: 0.29 ± 0.07 g, Winnie: 0.36 ± 0.03 g) and at 16-20 weeks (WT: 0.1 ± 0.03 g, *Ccr6*-/-: 0.63 ± 0.01 g, Winnie x *Ccr6*-/-: 0.5 ± 0.09 g, Winnie: 0.6 ± 0.09 g) a significant difference (****$p < 0.0001$) in the colon weight was observed between WT and Winnie x *Ccr6*-/-. The colon weight of Winnie x *Ccr6*-/- remained significantly lower (*$p < 0.05$) than that of Winnie, at 8 weeks but not at the second time point.

3.1.3 Colon Weight/Colon Length Ratio

The colon weight/colon length ratio was calculated at 8 weeks (WT: 0.018 ± 0.003, *Ccr6*-/-: 0.018 ± 0.002, Winnie x *Ccr6*-/-: 0.036 ± 0.008, Winnie: 0.041 ± 0.004) and at 16-20 weeks (WT: 0.01 ± 0.003, *Ccr6*-/-: 0.07 ± 0.011, Winnie x *Ccr6*-/-: 0.05 ± 0.009, Winnie: 0.06 ± 0.011). As shown in figure 1A, and the colon weight/colon length ratio was found to be significantly increased in Winnie and Winnie x *Ccr6*-/- compared to the WT. $p \leq 0.01$ (**), $p \leq 0.001$ (***) and $p \leq 0.0001$ (****).

3.1.4 Colon Weight/Body Weight Ratio

The colon weight to body weight ratio was calculated at 8 weeks (WT: 0.006 ± 0.001, *Ccr6*-/-: 0.007 ± 0.001, Winnie x *Ccr6*-/-: 0.017 ± 0.005, Winnie: 0.018 ± 0.002) and at 16-20 weeks (WT: 0.007 ± 0.001, *Ccr6*-/-: 0.026 ± 0.003, Winnie x *Ccr6*-/-: 0.023 ± 0.005, Winnie: 0.03 ± 0.004). As shown in figure 1B, and the colon weight/body weight ratio was found to be significantly increased [$p<0.0001$(****)] in Winnie and Winnie x *Ccr6*-/- compared to the WT.

3.1.5 Gross Colon Morphology

As shown in figure 1D (1-4), the observation of colon morphology and faecal contents at 16-20 weeks showed the faecal pellets were well -formed, solid and hard with no inflammation in the healthy control. Winnie x *Ccr6*-/- had semisolid faeces, no diarrhoea, faecal pellets formed in the distal colon, shows an intermediate level of milder inflammation to both positive control and healthy control where the proximal colon was more susceptible to inflammation but not the distal colon. Winnie had watery stools, diarrhoea, no occult, faecal pellets not formed, colitis and high inflammation during late disease.

3.2 Multi-System Pathophysiology

3.2.1 Colon Histology

Histological staining of colon tissue with H&E as shown in figure 1 C (1-4), revealed normal tissue architecture with no inflammation in WT and *Ccr6*-/- at 16-20 weeks of age. Winnie x *Ccr6*-/- displayed histological evidence of having less severe inflammation at pre and post-acute disease compared to Winnie, consistent with the fact that milder inflammation was seen in the proximal colon while the distal colon was free of inflammation. Attenuated colitis initiated by *Ccr6*-deficiency was indicated in Winnie x *Ccr6*-/-, showed increased goblet cell distribution with high mucus production compared to Winnie. *Ccr6*- deficiency appeared to stimulate more epithelial mucus secretion which had contributed to reduce inflammation. Severe inflammation seen in Winnie at 16-20 weeks was not observed in Winnie x *Ccr6*-/- to

Preprints (www.preprints.org) | NOT PEER-REVIEWED | Posted: 18 December 2019 doi:10.20944/preprints201912.0238.v1

that extent. Except for moderate immune cell infiltration and an occasional crypt abscess, Winnie x *Ccr6*-/- did not show deformed crypt architecture whereas prominent crypt abscesses, sporadic mucosal ulceration, epithelial hyperplasia and loss of goblet cells were observed in Winnie.

3.2.2 Spleen Weight

No significant difference existed in the mean spleen weight among the four genotypes at 8 weeks (WT: 0.07 g ± 0.004, *Ccr6*-/- 0.066 g ± 0.002, Winnie X *Ccr6*-/- 0.082 g ± 0.008, Winnie: 0.088 g ± 0.014). A significant difference (**p<0.01) was noted at 16-20 weeks of age (WT 0.09 g ± 0.007, *Ccr6*-/- 0.11 g ± 0.002, Winnie X *Ccr6*-/- 0.12 g ± 0.008 and Winnie 0.16 g ± 0.024) between WT and Winnie. Winnie X *Ccr6*-/- recorded a mean spleen weight intermediate to the WT and Winnie, during the second time point (figure 2A-B). $p \leq 0.01$ (**), $p \leq 0.001$ (***) and $p \leq 0.0001$ (****).

3.2.3 Spleen Histology

At 8 weeks of age, the spleen in the WT and *Ccr6*-/- appeared normal. A considerably high neutrophil reaction was evident in the red pulp in Winnie which indicated high inflammation. In contrast, Winnie x *Ccr6*-/- displayed a markedly lower neutrophil reaction in the red pulp with occasional neutrophil presence. At 16-20 weeks [figure 2C (1-4)] neutrophil infiltration in the spleen was observed even in the WT but it was significantly higher in Winnie with high extra medullary hemopoiesis reaction. A similar high neutrophil reaction was also noticeable in Winnie x *Ccr6*-/- at the latter time point of acute disease. An increased number of megakaryocytes were observed in Winnie spleen. The spleen consists of two distinctive areas named as white pulp and red pulp. White pulp is material which forms part of the immune system (lymphatic tissue) mainly made up of white blood cells. Red pulp is made up of blood-filled cavities (venous sinuses) and splenic cords (15).

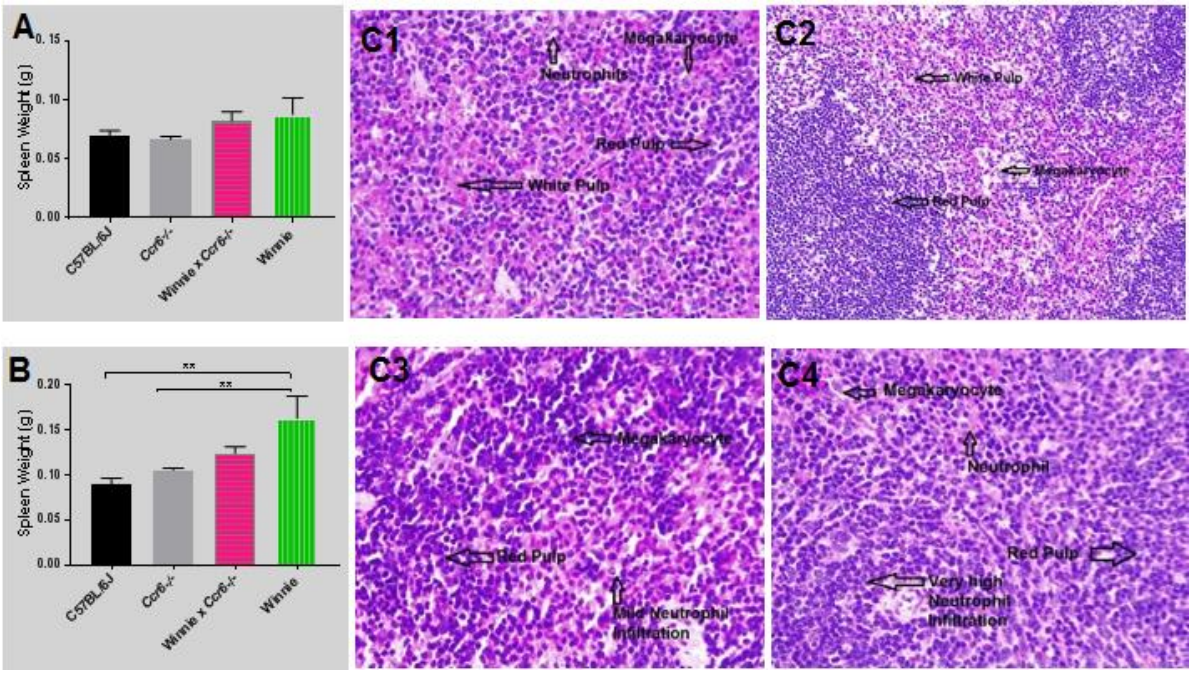

Preprints (www.preprints.org) | NOT PEER-REVIEWED | Posted: 18 December 2019 doi:10.20944/preprints201912.0238.v1

Figure 2. Comparison of spleen weight in the four genotypes (A) at 8 weeks of age and (B) at 16-20 weeks of age. Data expressed as mean ± SEM by repeated measures analysis of variance (ANOVA) and Tukey's multiple comparison test, n=7. $p \leq 0.01$ (**), $p \leq 0.001$ (***) and $p \leq 0.0001$ (****). (C) H&E sections of spleen histology at 16-20 weeks of age 1- WT, 2- *Ccr6-/-*, 3 -Winnie x *Ccr6-/-*, 4- Winnie at magnification x 200.

3.2.4 Liver Weight

The mean liver weight in the four genotypes, showed no significant difference at 8 weeks with the *Ccr6*-deficient model having the lowest mean weight (WT 1.275 ± 0.04 g, *Ccr6-/-* 1.114 ± 0.07 g, Winnie X *Ccr6-/-* 0.962 ± 0.11 g, Winnie 1.209 ±0.12 g). At 16-20 weeks, the mean liver weights were, WT 0.98 ± 0.04 g, *Ccr6-/-* 1.17 ± 0.05 g, Winnie X *Ccr6-/-* 1.48 ± 0.07 g, Winnie 1.54 ± 0.07 g while the mean liver weight of Winnie x *Ccr6-/-* was lower than that of Winnie (figure 3).

3.2.5 Liver Histology

No inflammation was detected in the liver of the WT at 16-20 weeks however, a larger collection of inflammatory cells was observed in hepatic lobules indicative of focal lobular inflammation in Winnie and *Ccr6-/-* mice, although not in the portal tracts. A smaller collection of mononuclear cells was present within the hepatic lobules in Winnie x *Ccr6-/-* identified as occasional neutrophils, eosinophils and other cells of lymphoid origin as evidenced in figure 3.

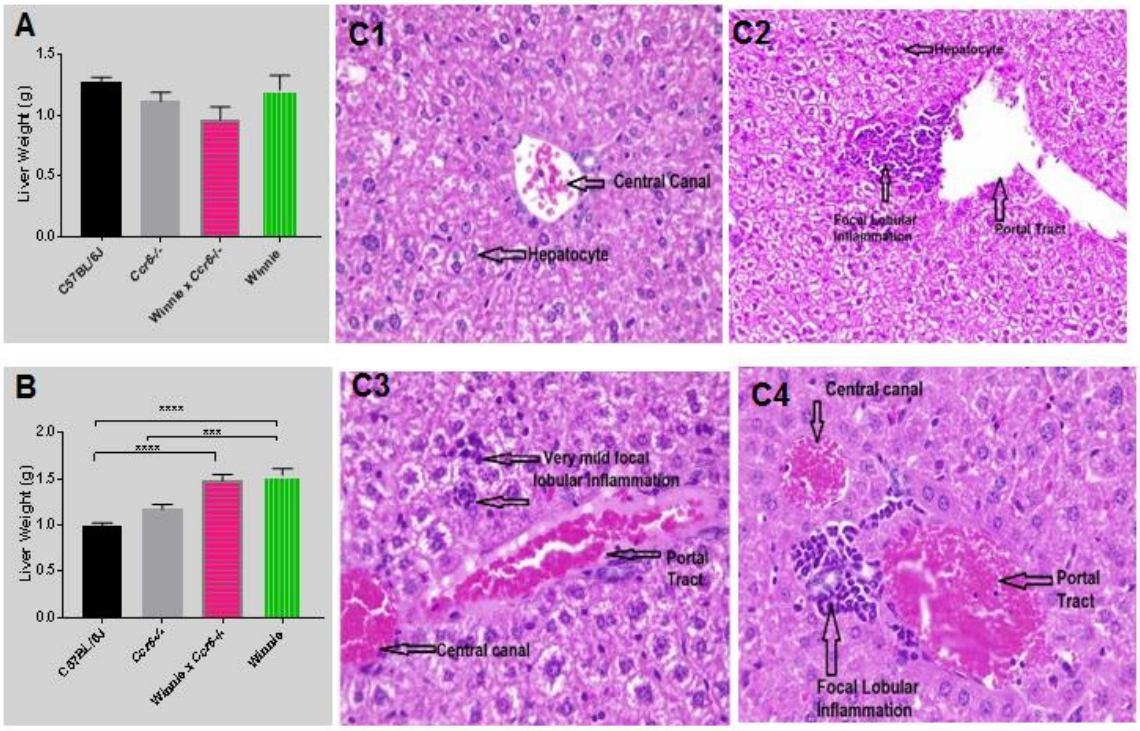

Figure 3. Comparison of liver weight in the four genotypes (A) at 8 weeks of age and (B) at 16-20 weeks of age. Data expressed as mean ± SEM by repeated measures analysis of variance (ANOVA) and Tukey's multiple comparison test, n=7. $p \leq 0.01$ (**), $p \leq 0.001$ (***) and $p \leq 0.0001$

Preprints (www.preprints.org) | NOT PEER-REVIEWED | Posted: 18 December 2019 doi:10.20944/preprints201912.0238.v1

(****). (C) H&E sections of liver histology at 16-20 weeks of age 1- WT, 2- *Ccr6*-/-, 3 -Winnie x *Ccr6*-/-, 4- Winnie at magnification x 200.

3.2.6 Kidney Weight

The mean renal weight (of both kidneys) at 8 weeks exhibited a significant difference among the four genotypes; WT: 0.310 ± 0.011 g, *Ccr6*-/-: 0.294 ± 0.017 g, Winnie x *Ccr6*-/-: 0.275 ± 0.033 g, Winnie 0.391 ± 0.013 g with the *Ccr6*-deficient model showing an intermediate value compared to WT and Winnie. At the 16-20 weeks, (WT: 0.28 ± 0.017 g, *Ccr6*-/-: 0.33 ± 0.019 g, Winnie x *Ccr6*-/-: 0.36 ± 0.021 g, Winnie: 0.43 ± 0.041 g) a significant difference [p<0.01 (****)] in renal weight existed between WT and Winnie (figure 4).

3.2.7 Kidney Histology

As shown in figure 4 C (1-4), no renal pathology was detectable in the kidneys of the four genotypes, 1- WT, 2- *Ccr6*-/-, 3- Winnie x *Ccr6*-/- and 4- Winnie, all of which showed normal renal histology. No signs of immune cells infiltration in the kidneys were detected by histology.

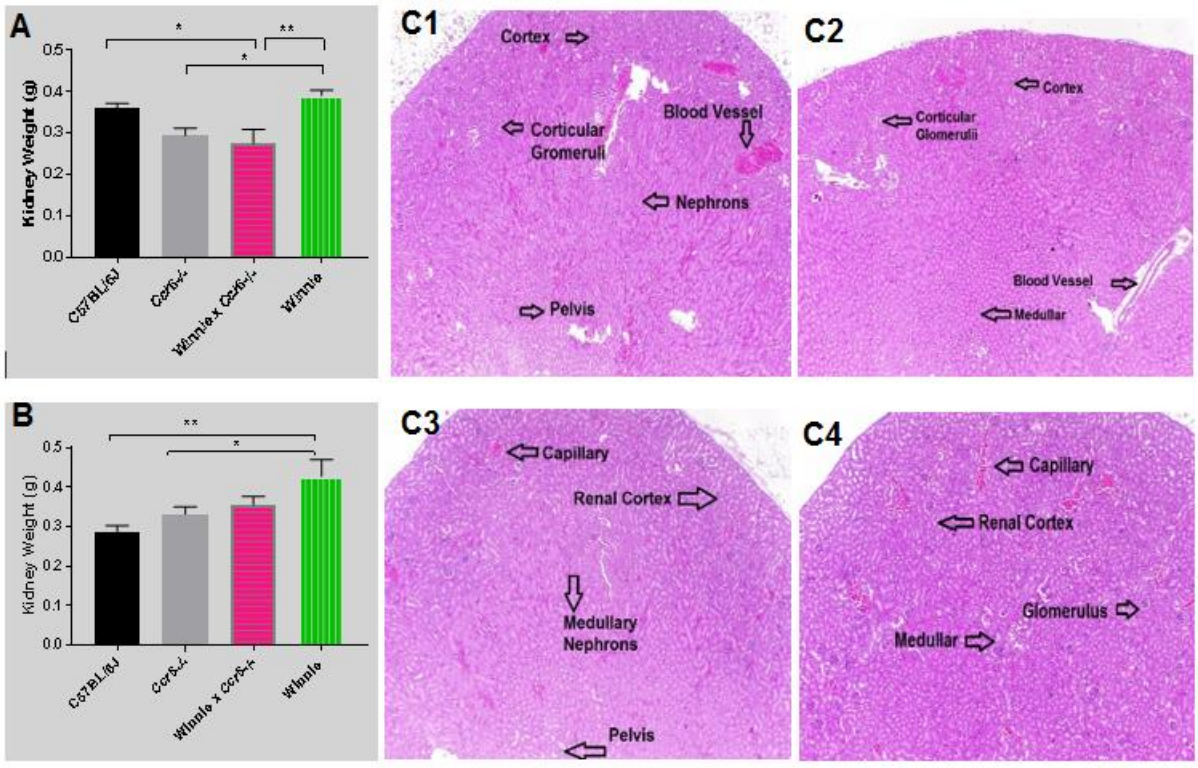

Figure 4. Comparison of kidney weight in the four genotypes (A) at 8 weeks of age and (B) at 16-20 weeks of age. Data expressed as mean ± SEM by repeated measures analysis of variance (ANOVA) and Tukey's multiple comparison test, n=7. p ≤ 0.01 (**), p ≤ 0.001 (***) and p ≤ 0.0001 (****). (C) H&E sections of kidney histology at 16-20 weeks of age 1- WT, 2- *Ccr6*-/-, 3 -Winnie x *Ccr6*-/-, 4- Winnie at magnification x 100.

Preprints (www.preprints.org) | NOT PEER-REVIEWED | Posted: 18 December 2019 doi:10.20944/preprints201912.0238.v1

3.3 Lymphocyte Distribution in the Spleen

3.3.1 Gating Strategy

The gating strategy used to quantify the lymphocyte percentages in the four genotypes in the spleen is displayed in figure 5. In order to investigate the relative distribution of T and B lymphocytes in the spleen, the percentages of the major surface markers (CD4, CD8 and CD19), were quantified by flowcytometry.

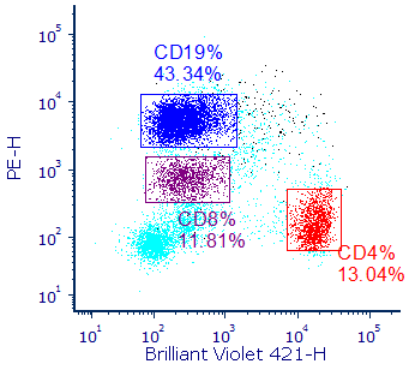

Figure 5: After gating the singlet cell population on FSC-H vs FSC-A axes, to discriminate against the doublets, CD4% gated in red, CD8% gated in maroon and CD19% gated in blue. Over 95% of the cell population remained viable at point of analysis.

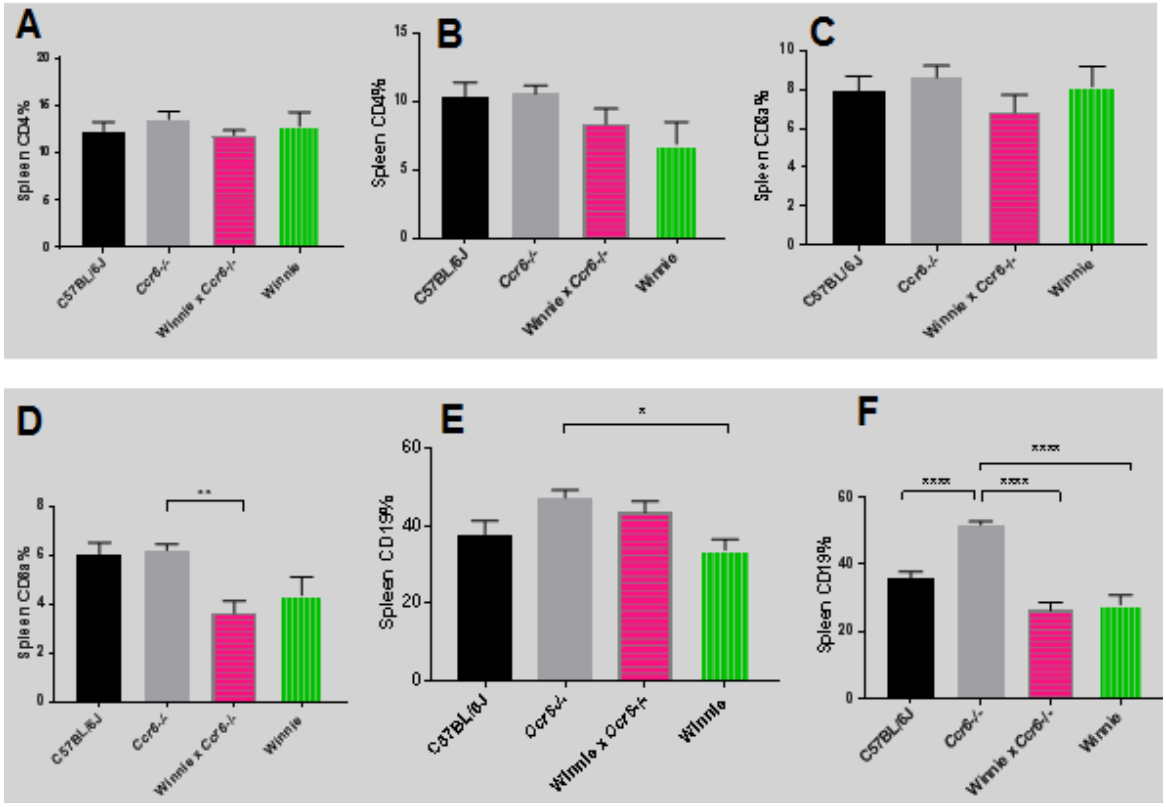

Preprints (www.preprints.org) | NOT PEER-REVIEWED | Posted: 18 December 2019 doi:10.20944/preprints201912.0238.v1

Figure 6: Comparison of CD4, CD8 and CD19 distribution in the spleen in the four genotypes at 8 weeks of age and 16-20 weeks of age by flowcytometry. No significant difference seen among the genotypes in the CD4 (A, B) and CD8 lymphocyte % (C, D) in the spleen with a rise in CD19% (E, F) in the *Ccr6*-deficient models, during early inflammatory stage. A trend of marked decline in all 3 surface markers is seen in the older diseased groups (B, D, F) where Winnie X *Ccr6*-/- % is intermediate to that of the healthy control and Winnie. n =7. Data expressed as mean ± SEM by repeated measures analysis of variance (ANOVA) and Tukey's multiple comparison test. **p<0.01. *** p<0.001, ****p<0.0001

3.3.2 T (CD4 & CD8) and B (CD19) lymphocyte distribution in the spleen.

As shown in figure 6, the spleen CD4 percentage (%) at both time points show negligible difference among the four genotypes tested. At 8 weeks the mean CD4 % splenic values were; WT: 12.4 ± 0.9, *Ccr6*-/-: 13.55 ± 0.8, Winnie x *Ccr6*-/-: 11.87 ± 0.5, Winnie: 12.81 ± 1.5 and at 16-20 weeks, WT: 10.3 ± 2.6, *Ccr6*-/-: 10.54 ± 1.8, Winnie x *Ccr6*-/-: 8.34 ± 2.8, Winnie: 7.0 ± 3.9. A similar trend of declining CD4% values is seen in the diseased models compared to WT at both time points. CD8 % in the spleen too is non-significant among the genotypes at (A) 8 weeks (WT: 7.93 ± 0.76, *Ccr6*-/- : 8.62 ± 0.61, Winnie x *Ccr6*-/-: 6.83 ± 0.91, Winnie: 8.15 ± 1.03) and at (B) 16-20 weeks, CD8 % were, WT: 6.0 ± 0.48, *Ccr6*-/-: 6.19 ± 0.24, Winnie x *Ccr6*-/-: 3.61 ± 0.51, Winnie 4.35 ± 0.75. Splenic CD19 % at (A) 8 weeks (WT: 37.87 ± 3.4, *Ccr6*-/-: 47.33 ± 2.0, Winnie x *Ccr6*-/-: 43.51 ± 2.8, Winnie: 33.75 ± 2.7 and during the (B) 16-20 weeks WT: 35.87 ± 1.9, *Ccr6*-/-: 51.72 ± 1.07, Winnie x *Ccr6*-/-: 26.22 ± 2.4, Winnie: 28.0 ± 2.9. Winnie x *Ccr6*-/- at both time points display reduced T and B cell production in the spleen, which may be considered a favourable outcome because lowered lymphocyte production in the spleen could result in reduced effector lymphocyte deployment from the spleen to the colon.

3.3.3 T (CD4 & CD8) and B (CD19) lymphocyte distribution in the Mesenteric Lymph Nodes (MLN).

The CD4% in MLN lymphocyte distribution (A) at 8 weeks; WT: 10.2 ± 0.08, *Ccr6*-/-: 13.93 ± 0.1, Winnie x *Ccr6*-/-: 6.26 ± 0.27, Winnie: 16.62 ± 0.16 (B) at 16-20 weeks; WT: 4.66 ± 0.04, *Ccr6*-/-: 30.77 ± 0.51, Winnie x *Ccr6*-/-: 22.19 ± 1.27, Winnie: 22.94 ± 0.07 (figure 7). Due to markedly reduced inflammation, the T and B lymphocytes in MLN of Winnie x *Ccr6*-/- displays decreased proliferation during both time points compared to the WT and Winnie. CD8 % at 8 weeks (C); WT: 13.5 ± 0.47, *Ccr6*-/-: 6.93 ± 0.08, Winnie x *Ccr6*-/-: 5.64 ± 0.08, Winnie: 15.8 ± 0.15 and at 16-20 weeks (D); WT: 3.65 ± 0.03, *Ccr6*-/-: 15.74 ± 0.65, Winnie x *Ccr6*-/-: 14.87 ± 0.55, Winnie: 18.38 ± 0.72. CD19 % (E) at 8 weeks; WT: 13.0 ± 0.29, *Ccr6*-/-: 17.0 ± 0.35, Winnie x *Ccr6*-/-: 6.47 ± 0.24, Winnie: 17.2 ± 0.3, (F) at 16-20 weeks; WT: 4.31 ± 0.13, *Ccr6*-/-: 34.18 ± 0.12, Winnie x *Ccr6*-/-: 37.69 + 1.1, Winnie: 39.65 ± 0.76.

Preprints (www.preprints.org) | NOT PEER-REVIEWED | Posted: 18 December 2019 doi:10.20944/preprints201912.0238.v1

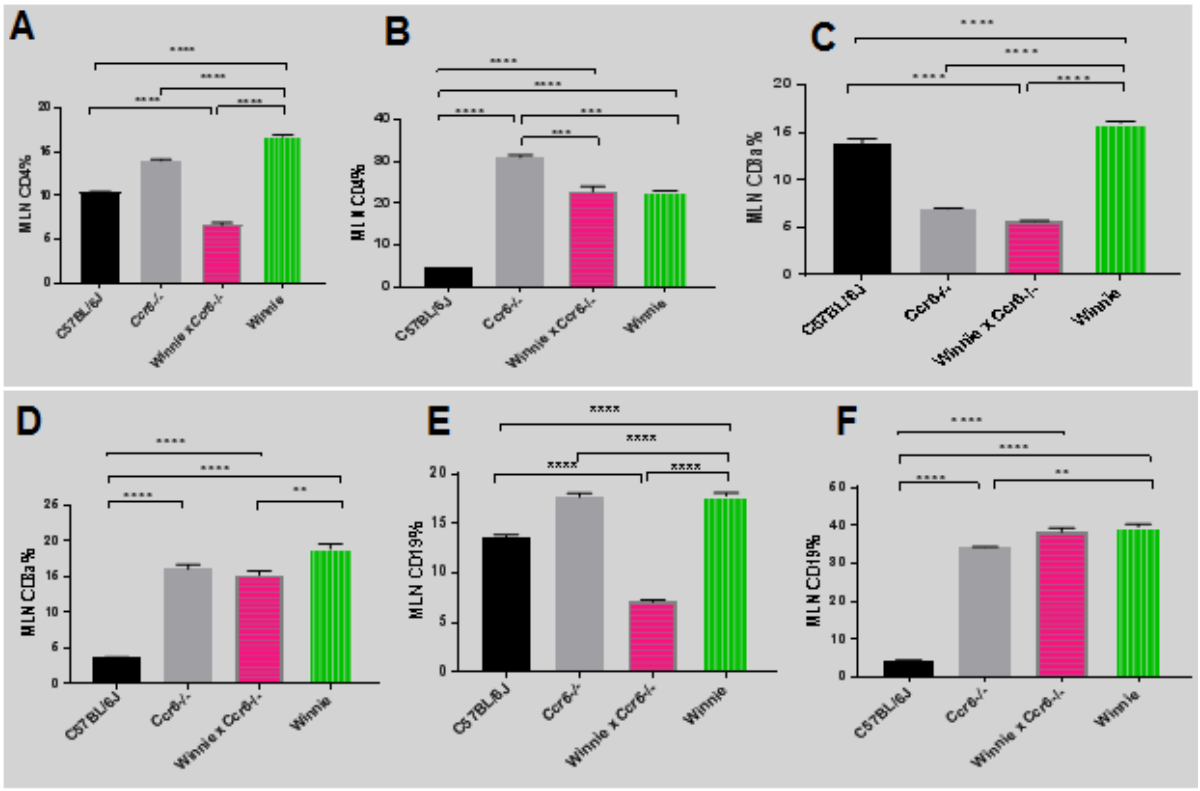

Figure 7: Comparison of CD4, CD8 and CD19 percentages in the mesenteric lymph nodes (MLN) in the four genotypes at 8 weeks (A, C, E) of age and 16-20 weeks (B, D, F) of age by flowcytometry. Data expressed as mean ± SEM by repeated measures analysis of variance (ANOVA) and Tukey's multiple comparison test, n=3. **p<0.01. *** p<0.001, ****p<0.0001

3.4 Molecular Signalling

3.4.1 CCL20 expression pattern in the colon.

As shown in figure 8 (A – D), a qualitative analysis of CCL20 expression pattern in the colon was made to identify the effect of the CCR6-CCL20 axis on the gut immune mechanisms during spontaneous colitis using IHC (16). CCL20 expression pattern at 16-20 weeks of age in the four genotypes were WT: 0.006 ± 0.0003, *Ccr6*-/-: 0.012 ± 0.0003, Winnie x *Ccr6*-/-: 0.012 ± 0.0003, Winnie: 0.015 ± 0.0003.

3.4.2 Phosphorylated Akt (Akt^P) expression pattern in the colon.

As shown in figure 8 (E-H), a qualitative analysis of phosphorylated Akt (Akt^P) expression pattern in the colon was made to identify the molecular signalling stimulated by the CCR6-CCL20 axis on the gut immune mechanisms during spontaneous colitis using IHC. The Akt^P expression at 16-20 weeks in the four genotypes were WT: 0.007 ± 0.0003, *Ccr6*-/-: 0.009 ± 0.0005, Winnie x *Ccr6*-/-: 0.02 ± 0.001, Winnie: 0.015 ± 0.0003.

Preprints (www.preprints.org) | NOT PEER-REVIEWED | Posted: 18 December 2019 doi:10.20944/preprints201912.0238.v1

3.4.3 Phosphoinositide 3-kinase (PI3K) expression pattern in the colon.

As shown in figure 8 (I-L), a qualitative analysis of PI3K expression pattern in the colon as shown in figure 24 was made to identify the molecular signalling stimulated by the CCR6-CCL20 axis on the gut immune mechanisms during spontaneous colitis using IHC. The expression pattern of PI3K values at 16-20 weeks of age, in the four genotypes were WT: 0.05 ± 0.001, *Ccr6* -/-: 0.011 ± 0.001, Winnie X *Ccr6*-/-: 0.014 ± 0.0003, Winnie: 0.029 ± 0.001.

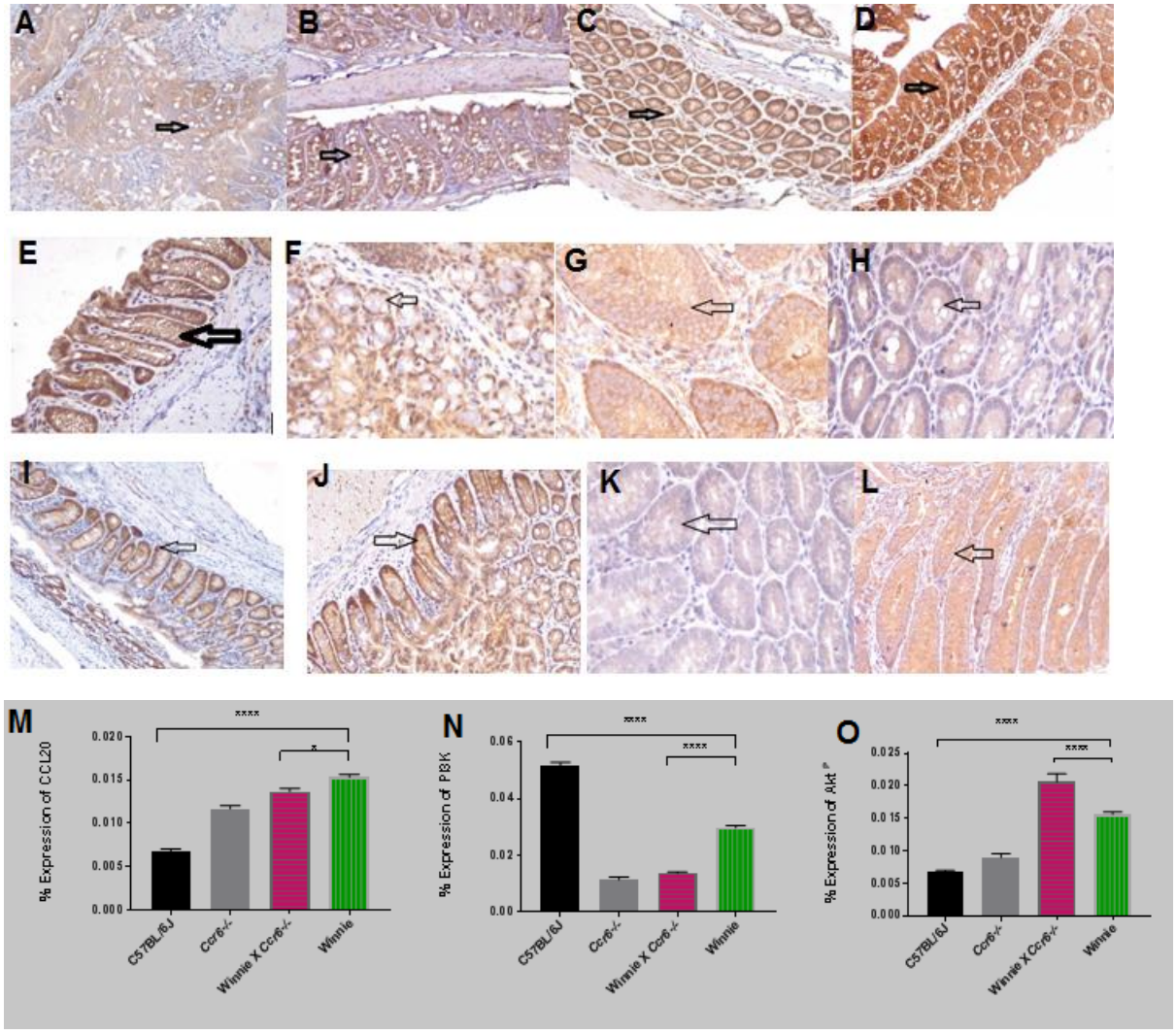

Figure 8: Comparison of the CCL20 (A-D), PI3K (E-H) and phosphorylated Akt (I-L) distribution in the colon in the four genotypes at 16-20 weeks. Arrow indicates brown colour which determines the presence of DAB chromogen bound to anti-CCL20 -anti-mouse primary antibody, magnified at x200. The % expression of CCl20 (M), PI3K (N) and phosphorylated Akt (O) quantified by Fiji image J software showing increased CCL20 and Akt^{P} expression in the colon with a significant decrease in PI3K expression in Winnie x Ccr6-/- compared to WT. In all three measurements made between Winnie x Ccr6-/- and Winnie, a significant reduction in these biomolecules was detected in the *Ccr6*-deficient Winnie.

Preprints (www.preprints.org) | NOT PEER-REVIEWED | Posted: 18 December 2019 doi:10.20944/preprints201912.0238.v1

3.5 Immunological Parameters

The cytokine mRNA expression in colon tissue (Table 2) was quantified in the four genotypes and a decrease in the mRNA fold change expression normalised to the WT was observed in Winnie x *Ccr6*-/-. In most cytokines at both time points, Winnie x *Ccr6*-/- readings were lower than that of Winnie. CD is characterised by TH1 cytokines, particularly Interferon-gamma (IFN-γ), Tumour necrosis factor- alpha (TNF-α), Interleukin -18 (IL-18) and Interleukin-12 (IL-12). UC is considered as having a TH2-like cytokine profile including Interleukin-4 (IL-4), Interleukin-6 (IL-6) and Interleukin -13 (IL-13), all of which reduced disease severity in various mouse models and humans when blocked with antibodies of the respective TH1 and TH2 cytokine milieu (17).

TH1	TH2	TH17	Treg	Other
IFN-g	IL-4	IL-17A	IL-10	AHR
TNF-a	IL-6	IL-23R		CCL20
IL-18	IL-13			

Table 2: The cytokine expression evaluated by RT-PCR, divided into respective immune responses of the T helper lymphocyte populations.

Cytokine mRNA expression	Fold change normalized to WT	Fold change in Ccr6-/- at 8 wks	Fold change in Ccr6-/- at 16-20 wks	Fold change in Winnie X Ccr6-/- at 8 wks	Fold change in Winnie X Ccr6-/- at 16-20 wks	Fold change in Winnie at 16-20 wks	Fold change in Winnie at 16-20 wks
IFN-g	**1.0**	**0.8**	**2.5**	**0.5**	**3.0**	**6.0**	**3.0**
TNF-a	**1.0**	**0.3**	**1.0**	**0.3**	**3.0**	**5.0**	**3.5**
IL-18	**1.0**	**1.0**	**10.0**	**1.8**	**4.0**	**14.0**	**10.0**
IL-4	**1.0**	**0.3**	**0.5**	**0.5**	**2.0**	**14.0**	**8.0**
IL-6	**1.0**	**0.5**	**1.0**	**2.0**	**1.0**	**8.0**	**2.0**
IL-13	**1.0**	**0.3**	**1.0**	**2.0**	**2.0**	**14.0**	**2.0**
IL-17A	**1.0**	**1.0**	**1.0**	**0.8**	**0.8**	**14.0**	**1.5**
IL-23R	**1.0**	**0.3**	**0.3**	**1.0**	**2.0**	**14.0**	**2.0**
IL-10	**1.0**	**2.0**	**2.5**	**1.0**	**4.0**	**14.0**	**4.0**
AHR	**1.0**	**0.3**	**2.0**	**2.0**	**2.5**	**8.0**	**1.8**

Table 3: The fold change increase or decrease in mRNA expression of the cytokines tested, normalized to WT. Winnie at both time points, recorded the highest mRNA expression in all 9 cytokines in the colon. Increase is shown in blue colour code. A decrease in cytokine expression, highlighted in yellow, was noted in *Ccr6*-/-. Winnie X *Ccr6*-/- showed a moderate increase in cytokine levels, during disease progression compared to WT and Winnie highlighted by blue colour. Red colour indicates equality to WT, in most of the cytokines in *Ccr6*-/- and Winnie X *Ccr6*-/- during early onset of inflammation. Interestingly the cytokine expression in CCR6-deficient Winnie was always lower than those of Winnie, which enables us to understand the low level of inflammation presented in our study model.

Preprints (www.preprints.org) | NOT PEER-REVIEWED | Posted: 18 December 2019 doi:10.20944/preprints201912.0238.v1

3.5.1 TH1 cytokine mRNA expression in the colon.

In order to evaluate the TH1 cytokine expression in the colon of the four genotypes, the relative fold change in mRNA expression normalised to WT, was quantified by RT-PCR (figure 9, table 3). The TH1 cytokine profile included Interferon-gamma (IFN-γ), Tumour necrosis factor-alpha (TNF-α), Interleukin-18 (IL-18) mRNA expression at 8 weeks and 16-20 weeks of age. The IFN- γ values at 8 weeks were (WT: 1.0 ± 0, *Ccr6*-/-: 0.7 ± 0.2, Winnie x *Ccr6*-/-: 1.0 ± 0.8, Winnie: 10.0 ± 4.5) and at 16-20 weeks (WT: 1.0 ± 0, *Ccr6*-/-: 2.0 ± 1.0, Winnie x *Ccr6*-/-: 3.0 ± 1.0, Winnie: 3.0 ± 1.5). TNF-α values at 8 weeks were (WT: 1.0 ± 0, *Ccr6*-/-: 1.0 ± 0.45, Winnie x *Ccr6*-/-: 2.0 ± 1.8, Winnie: 10 ± 2.5) and at 16-20 weeks (WT: 1.0 + 0, *Ccr6*-/-: 1.0 ± 0.3, Winnie x *Ccr6*-/-: 3.0 ± 2.2, Winnie: 4.0 ± 3.6). IL-18 values at 8 weeks were (WT: 1.0 ± 0, *Ccr6*-/-: 2.25 ± 1.0, Winnie x *Ccr6*-/-: 10.0 ± 1.8, Winnie: 39.0 ± 1.0) and at 16-20 weeks (WT: 1 ± 0, *Ccr6*-/-: 12.0 ± 5.8, Winnie x *Ccr6*-/-: 5.0 ± 3.4, Winnie: 12.0 ± 5.8). Winnie x *Ccr6*-/- readings were found to be lower than that of the positive control in all the cytokines at both time points.

3.5.2 TH2 cytokine mRNA expression in the colon.

The TH2 cytokine expression in the colon of the four genotypes, the relative fold change in mRNA expression normalised to WT, was quantified by RT-PCR (figure 9, table 3). The TH2 cytokine profile included Interleukin 4 (IL-4), Interleukin 6 (IL-6) and Interleukin 13 (IL-13) mRNA expression at 8 weeks and 16-20 weeks of age. IL-4 values at 8 weeks; WT: 1.0 ± 0, *Ccr6*-/-: 0.3 ± 0.11, Winnie x *Ccr6*-/-: 1.0 ± 0.8, Winnie: 35.0 + 1.0 and at 16-20 weeks; WT: 1.0 ± 0, *Ccr6*-/-: 0.5 ± 0.06, Winnie x *Ccr6*-/-: 5.0 ± 3.5, Winnie: 8.0 ± 5.6. IL-6 values at 8 weeks; WT: 1.0 ± 0, *Ccr6*-/-: 0.4 ± 0.1, Winnie x *Ccr6*-/-: 3.0 ± 2.2, Winnie: 9.0 ± 1.0, and at 16-20 weeks; WT: 1.0 ± 0, *Ccr6*-/-: 1.0 ± 0.5, Winnie x *Ccr6*-/-: 1.0 ± 0, Winnie: 3.0 ± 2.0. IL-13 values at 8 weeks; WT: 1.0 ± 0, *Ccr6*-/-: 0.3 ± 0, Winnie x *Ccr6*-/-: 2.0 ± 1.0, Winnie: 22.0 ± 1.0 and at 16-20 weeks; WT: 1.0 ± 0, *Ccr6*-/-: 1.0 + 0, Winnie x *Ccr6*-/-: 4.0 ± 1.5, Winnie: 4.0 ± 1.0. Winnie x *Ccr6*-/- readings were found to be lower than that of the positive control in all the cytokines at both time points.

3.5.3 TH17 cytokine mRNA expression in the colon.

The TH17 cytokine expression in the colon of the four genotypes, the relative fold change in mRNA expression normalised to WT, was quantified by RT-PCR. As shown in figure 9, and table 3, the TH17 cytokine profile included Interleukin 17A (IL-17A) and Interleukin 23 Receptor (IL-23R) mRNA expression at 8 weeks and 16-20 weeks of age. IL-17 A values at 8 weeks; WT: 1.0 ± 0, *Ccr6*-/-: 1.0 ± 0.6, Winnie x *Ccr6*-/-: 2.0 ± 0, Winnie: 35.0 ± 1.0 and at 16-20 weeks; WT: 1.0 ± 0, *Ccr6*-/-: 1.0 ± 0.6, Winnie x *Ccr6*-/-: 2.0 ± 0, Winnie: 35.0 ± 1.0. IL-23R values at 8 weeks; WT: 1.0 ± 0, *Ccr6*-/-: 0.3 ± 0.2, Winnie x *Ccr6*-/-: 1.0 ± 0.3, Winnie: 62.0 ± 1.0 and at 16-20 weeks; WT: 1.0 ± 0, *Ccr6*-/-: 0.3 ± 0.15, Winnie x *Ccr6*-/-: 2.0 ± 1.8, Winnie: 2.0 ± 1.8. Winnie x *Ccr6*-/- readings were found to be lower than that of the positive control in all the cytokines at both time points.

3.5.4 Anti-inflammatory (Treg) cytokine mRNA expression in the colon.

As shown in figure 9, table 3, to evaluate the anti-inflammatory cytokine expression in the colon of the four genotypes, the relative fold change in mRNA expression of Interleukin 10 (IL-10) normalised to WT, was quantified by RT-PCR. The IL-10 cytokine profile at 8 weeks; (WT: 1.0 ± 0, *Ccr6*-/-: 2.0 ± 1.0, Winnie x *Ccr6*-/-: 1.0 ± 1.0, Winnie: 70.0 ± 1.0) and at 16-20 weeks

Preprints (www.preprints.org) | NOT PEER-REVIEWED | Posted: 18 December 2019 doi:10.20944/preprints201912.0238.v1

(WT: 1.0 ± 0, *Ccr6*-/-: 2.5 ± 1.0, Winnie x *Ccr6*-/-: 4.0 ± 1.5, Winnie: 4.0 ± 1.0). Winnie x *Ccr6*-/- reading was higher than that of the positive control at the second time point.

3.5.5 Anti-inflammatory (Aryl Hydrocarbon Receptor - AHR) cytokine in the colon.

The anti-inflammatory cytokine expression in the colon of the four genotypes, the relative fold change in mRNA expression of Aryl Hydrocarbon Receptor (AHR) normalised to WT, was quantified by RT-PCR. As shown in figure 9, table 3, the AHR cytokine profile at 8 weeks; (WT: 1.0 ± 0, *Ccr6*-/-: 0.4 ± 1.0, Winnie x *Ccr6*-/-: 3.0 ± 1.0, Winnie: 10.0 ± 1.0) and at 16-20 weeks were as follows; (WT: 1.0 ± 0, *Ccr6*-/-: 2.0 ± 1.0, Winnie x *Ccr6*-/-: 2.5 ± 1.5, Winnie: 1.8 ± 1.0). Winnie x *Ccr6*-/- reading was significantly (*** $p<0.001$) higher than that of the positive control at the second time point.

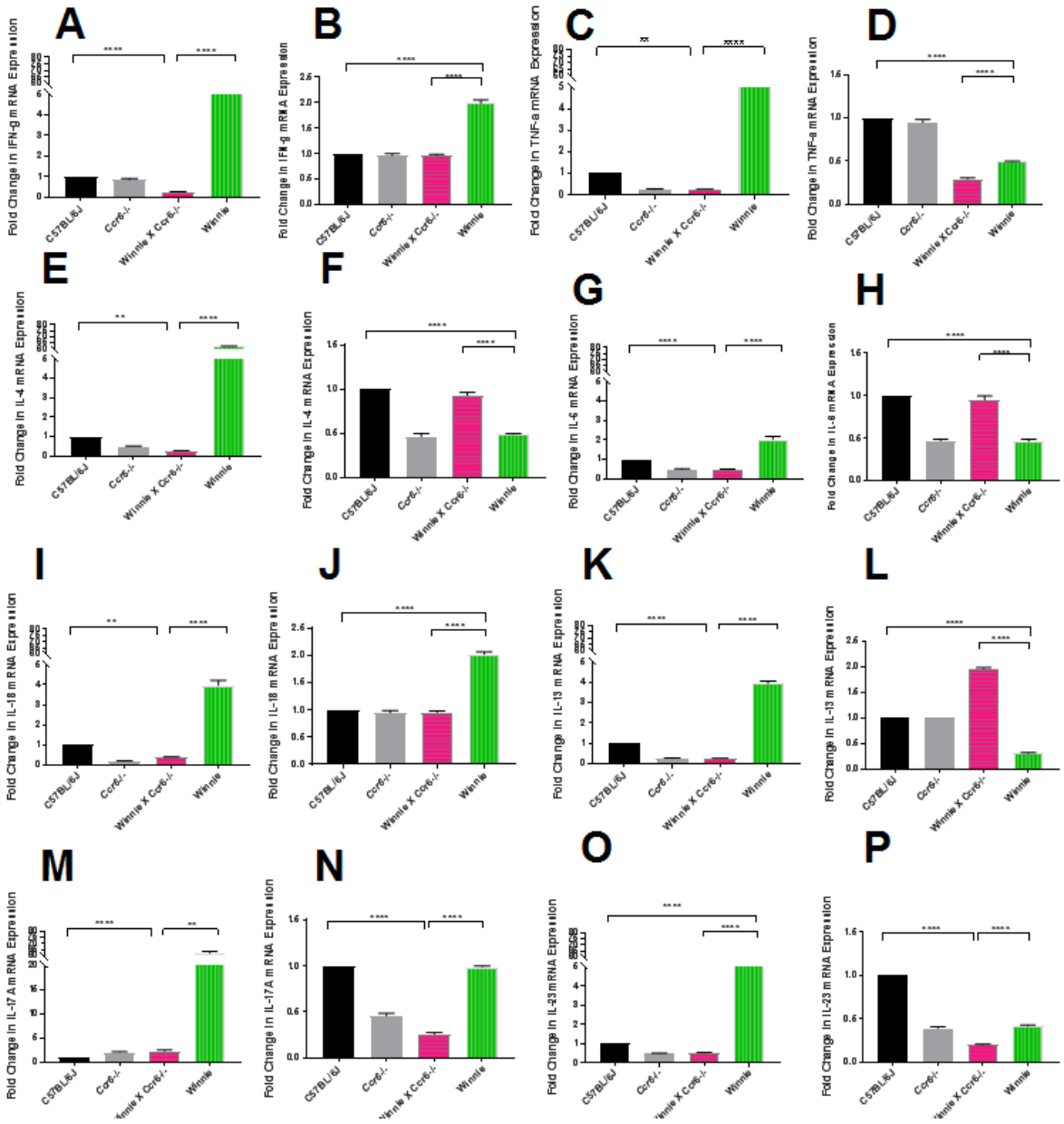

Preprints (www.preprints.org) | NOT PEER-REVIEWED | Posted: 18 December 2019 doi:10.20944/preprints201912.0238.v1

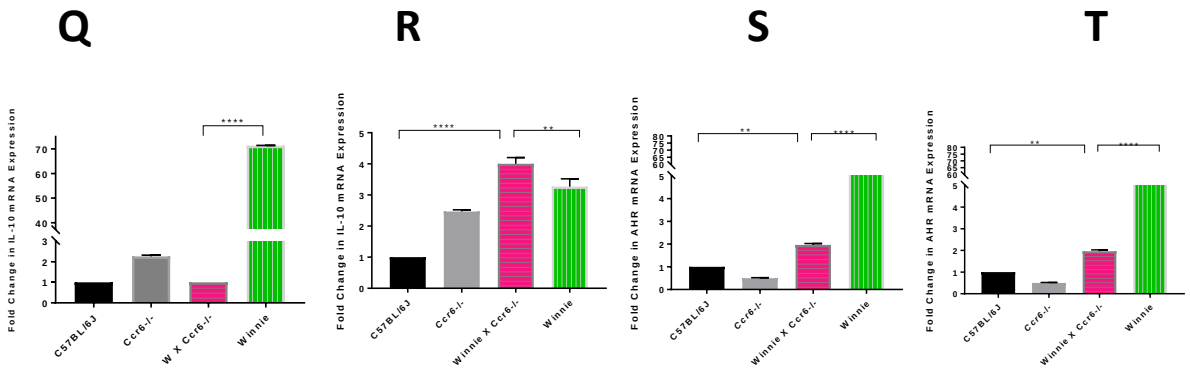

Figure 9:Fold change in mRNA expression of IFN-g (A,B), TNF-a (C, D), IL-4 (E,F), IL-6 (G,H),IL-18 (I,J), IL-13 (K,L), IL-17A (M,N), IL-23R (O,P), IL-10 (Q,R), AHR (S,T) at 8 weeks (A,E,I,M,Q, U) and C,G,K,O,S) and 16-20 weeks (B, F, J, N,R) and D, H, L, P T). Cycle of threshold (CT) values were normalised to *Gapdh* and CT calculated using the method of $2^{-\Delta CT}$. Data expressed as mean ± SEM by repeated measures analysis of variance (ANOVA) and Tukey's multiple comparison test, n=3. **p<0.01. *** p<0.001, ****p<0.0001

4.0 Discussion

The purpose of this investigation was to evaluate *Ccr6*-deficiency in multi-organ pathophysiology and its role in molecular signalling during the manifestation of spontaneous chronic colitis. The results of this study have revealed that CCR6 plays a pathogenic role during the development of chronic colitis. As a direct result of *Ccr6* -deficiency during the continuance of colitis in Winnie, the following salient features were observed; (i) distinct reduction in colonic inflammation, spleen and liver (ii) absence of renal pathology (iii) suppressed TH1, TH2, TH17 and Treg immune responses in the colon (iv) restrained production and egression of lymphocytes from the spleen (v) high lymphocyte proliferation within the mesenteric lymph nodes and (vi) increased production of CCL20, and Akt^{P} with decreased production of PI3K in the colon.

Both human and mice systems have provided evidence for the role played by CCR6-CCL20 axis in the progression and pathogenicity of several autoimmune disorders, as well as IBD (18). The study model used in this investigation, namely Winnie which carries a missense point mutation in the *Muc2* gene displays a similar but a relatively less severe intestinal inflammation that mimics human colitis. Winnie mouse model as a tool has multiple advantages in comparison to other contrived colitis models which include (i) chemically induced models such as DSS and TNBS induced colitis (no need for toxic chemicals) (ii) adoptive T cell transfer induced colitis (induced in an artificial immune deficient system) (iii) genetically engineered models of colitis (complete deficiency of immune functions) for the following reasons such as (i) disease manifests as spontaneous colitis, (ii) mimics human UC, (iii) doesn't cause severe tissue damage and (iv) it maintains an intact immune system resembling a normal immune system in comparison to T cell transfer models (12). Additionally, inflammation in Winnie naturally occurred at 6 weeks of age (2) and progressed with

Preprints (www.preprints.org) | NOT PEER-REVIEWED | Posted: 18 December 2019 doi:10.20944/preprints201912.0238.v1

age. Backcrossing Winnie to *Ccr6* deficient mice created a unique system that enabled us to study the role played by *Ccr6* in an established chronic colitis setting.

The *Ccr6*-deficient Winnie model demonstrated absence of weight loss, faecal occult blood, and diarrhoea with fully formed faecal pellets in the distal colon. An increase in wet colon weight and shortened colon length indicate elevated inflammation (19) due to fluid accumulation and thickening of the colon attributed to oedematous swelling and thickening of bowel wall. Colon weight to body weight ratio which is often treated as a quantitative index of colonic inflammation, when calculated, appeared to have reduced inflammation in Winnie x *Ccr6*-/- compared to Winnie. All the clinical parameters described above lead to the conclusion that *Ccr6* deficiency renders Winnie with reduced colitis. Our data is in complete agreement with results obtained by several research groups that have utilised the *Ccr6* deficient mouse systems. For example, *Ccr6*-deficient mice induced by DSS had displayed reduced susceptibility to the disease (20) while TNBS - induced colitis was attenuated by blocking the release of CCL20 (21). The adoptive transfer of $CCR6^+$ CD4 T cells into recipient recombination activation gene 2 (Rag2-/-) mice also caused aggravated disease (22).

The CCR6-CCL20 axis plays a pivotal role in maintaining immune homeostasis in the gut (17). It produces immune tolerance against the plethora of infectious luminal microbes which penetrate the gut mucosa and simultaneously step up immunity against many other disease-causing secondary contributing factors. When the purported immune tolerance breaks down, the phenomenal TH17 Vs Treg imbalance paradigm comes into play either by increased multiplication of pro-inflammatory immune cells such as $CCR6^+$TH17 and $CCR6^+$TH1, or by immune mechanisms that suppress the production of Treg cells (22). This scenario is empowered by CCR6 which mainly functions in the role of directing immune cell chemotaxis and thus stimulating a cascade of accessory molecules and cytokines.

The attenuation in inflammation was consistently evident in the colonic histomorphology (with increased goblet cell numbers which stimulated an increased production of mucus) seen in the study model in comparison to Winnie (which has deficient mucus generation). Features of acute disease histology were less prominent in Winnie x *Ccr6* -/- with all the general criteria used in the assessment such as epithelial hyperplasia, crypt abscesses, mucosal ulceration and immune cell infiltration being markedly reduced, showing a milder inflammatory status which correlated well with the clinical parameters.

In addition to having pathology within the gastrointestinal tract, IBD patients also exhibit secondary organ pathologies termed as extraintestinal manifestations (23). The spleen, liver and kidneys which are immune-related organs of secondary lymphoid origin were examined as they cause the systemic diseases - hepatitis and glomerular nephritis, where CCR6 plays a pivotal role in initiating inflammation (24), (25), (26), (27). Renal histology remained normal and unaffected by the *Ccr6*-gene ablation although there have been reports on *Ccr6* -deficiency having aggravated renal injury and increased mortality among nephritic mice because compared with the WT, *Ccr6* -deficiency in mice had

Preprints (www.preprints.org) | NOT PEER-REVIEWED | Posted: 18 December 2019 doi:10.20944/preprints201912.0238.v1

reduced infiltration of regulatory T cells (Treg cells) and TH17 cells but not the TH1 type (28).

In contrast to displaying normal kidney histology, liver pathology indicated significant lobular inflammation in Winnie with milder inflammation in the *Ccr6*-deficient Winnie (29). There are reports which describe the occurrence of concomitant hepatobiliary manifestations in IBD patients, of which the most common complication being primary sclerosing cholangitis (PSC) (30). Recent research findings have evaluated the presence of liver extrahepatic manifestations associated with IBD. Consistent with the mild inflammation seen in this study, there were no granulomas, hepatic abscesses, amyloidosis, and gallstones which are traditionally observed in CD, while PSC and autoimmune hepatitis are usually described in UC patients (30). One of the important observations made in this investigation is that *Ccr6*-deficiency serves to reduce the disease severity in the liver and spleen of colitis-afflicted mice.
The distribution of the major lymphocyte types in the spleen were ascertained with respect to *Ccr6* gene deficiency in order to highlight whether an immune-specific deficiency in the lymphocyte arm is created. CD4, CD8 and CD19 are major surface markers of the T and B lymphocyte repertoire in the spleen. Heightened inflammation in Winnie could be attributed to an imbalance in immune responses of T and B lymphocytes produced in the spleen because they are less in number. The impact of *Ccr6*-deficiency on lymphocyte production in the spleen produces suppressed effector cell mobilization and dysfunctional lymphocyte egression from the spleen. FTY720, an inhibitor of the sphingosine 1 phosphate receptor (SIP1) agonist has been shown to restrict CD4 T lymphocyte egression from lymph nodes during the disease course of allergic diarrhoea (31). *Ccr6* - deficiency in Winnie may possibly produce similar SIP1 receptor inhibition reactivity resulting in diminished CD4 lymphocyte egression from the spleen in Winnie during acute colitis.

IFN-γ, TNF-α and IL-18 are considered as pro-inflammatory cytokines in IBD. Published data have revealed a robust production of IFN-γ in the gut of DSS-treated WT mice associated with severe intestinal inflammation (32). Neutralization antibody against IFN-γ had partially but significantly ameliorated disease (33). IFN-γ which is regarded as a key TH1- upregulated - inflammatory cytokine, is also involved in regulating intestinal epithelial cell homeostasis, cell proliferation and apoptosis through converging beta- catenin signalling pathways (34), and activating the major histocompatibility complex class II (MHC II) on antigen-presenting cells and non-immune cells (35). The flip side of IFN-γ being a key inflammatory cytokine is that it bears anti-inflammatory properties too which may be supported by the observations made at the latter time point. It was shown in a mouse model of *Salmonella typhimurium*- induced colitis, that in animals lacking IFN-γ, the severity of intestinal inflammation was markedly attenuated (36). Moreover, IFN-γ has been identified as a negative regulator of IL-23 – mediated experimental colitis (37).

High levels of TNF-α in the intestinal mucosa is associated with the development of relapses and sustaining chronic inflammatory activity, which in this study model was markedly reduced. Intestinal homing of memory T lymphocytes were shown to augment TNF-α levels in relapsing UC patients along with higher

Preprints (www.preprints.org) | NOT PEER-REVIEWED | Posted: 18 December 2019 doi:10.20944/preprints201912.0238.v1

NF-KB nuclear translocation in lamina propria mononuclear cells taken from IBD patients (38).

The TH2 cells produce IL-4, IL-5, IL-6, IL-10 and IL-13 and promote atopy through activation of mast cells and induction of Ig E immune responses. IL-4, IL-10 and IL-13 are known to inhibit TH1-mediated immune responses (39) which have been clearly evident in *Ccr6*-deficient Winnie.

In this study, *Ccr6*-deficiency significantly induced a remarkably high IL-10 expression at 8 weeks, during early onset of inflammation. This may be one contributing factor which had favoured reduced inflammation shown by Winnie x *Ccr6*-/- during the acute disease phase. IL-10 is an established anti-inflammatory cytokine produced by T cells, B cells and monocytes when stimulated by an antigenic stimulus. IL-10 is known to downregulate MHC II molecules which diminish the antigen presenting capacity of cells thus inhibiting the production of IL-6, IL-1β and TNF-α (39).
IL-17 and IL-23 are potent inflammatory cytokines which induce opposing effects in colitis. Inhibition of IL-17 had exacerbated CD and weakened epithelial barrier integrity, thus exhibiting its potency for activating disease resolution. IL-23 inhibition had attenuated CD as well as promoting the development of the regulatory T cells (40). In another study, antibodies targeting IL-23 had ameliorated colitis (41). Results of this study are consistent with these observations because both IL-17A and IL-23 appear to perform dual roles in colitis.

The presence of phosphoinositide 3-kinase (PI3K) in the healthy control is due to PI3K activation by G-protein coupled receptor repertoire. PI3K is associated with a host of cellular activities including cell cycle, cell survival, cell proliferation etc. PI3K in Winnie and Winnie x *Ccr6*-/- models confirm that the AKT/mTOR pathway, NF-kB pathway, MAPK pathway, are upregulated inducing inflammation in the murine colon during spontaneous colitis (42). The PI3K pathway, has a critical signal transduction system linking oncogenes and multiple receptor classes to many essential cellular functions. It is perhaps the most commonly activated signalling pathway in human cancer (43). A remarkable fact is that the *Ccr6*-deficiency in Winnie had downregulated the PI3K expression in the colonic epithelial tissue.

Winnie x *Ccr6*-/- was shown to have the highest percentage expression in phosphorylated Akt, during late disease, from which we could possibly deduce it to behave as a favourable mediator which had contributed to reduce inflammation in murine colitis. Protein kinase B (PKB), also known as Akt, is a serine/threonine-specific protein kinase that plays a key role in multiple cellular processes such as glucose metabolism, apoptosis, cell proliferation, transcription and cell migration (44). Among the network of immune pathways associated with Akt (figure 10), the CCR6-stimulated Akt/mTOR signalling pathway leads to the activation of STAT3 which decisively selects the differentiation of T cells into TH17 and Treg populations in the gut (22).

The limitations of the study include lack of functional studies on the immune cell repertoires and quantification of regulatory T cells and other T lymphocyte cohorts as well as detailed screening of the proteins involved in molecular signalling. The inability to increase the number of samples tested from each genotype, particularly for cytokine evaluation due to

Preprints (www.preprints.org) | NOT PEER-REVIEWED | Posted: 18 December 2019 doi:10.20944/preprints201912.0238.v1

resource constraints is seen as a shortcoming.

Recent GWAS studies illustrated *Ccr6* as a predisposing genetic locus in IBD patients, a mechanism by which CCR6 imparts immunological modulation. This study has highlighted a functional role for CCR6 in the pathogenicity of spontaneous chronic colitis and provides a clue that CCR6 could be utilised as a functional therapeutic target in IBD. The proven functional efficacy in CCR6-inhibition in psoriasis, rheumatoid arthritis, multiple sclerosis carcinoma and EAE, could be replicated in IBD as well (1). Recent research had shown the direct involvement of CCR6 with AKT/mTOR pathway which contributes to the TH17/Treg imbalance which is considered as the prime immunological factor which decides the resolution of colitis (22). In conclusion, it is proposed to further evaluate the potency of CCR6 - inhibition as an active drug target in the clinical studies of colitis.

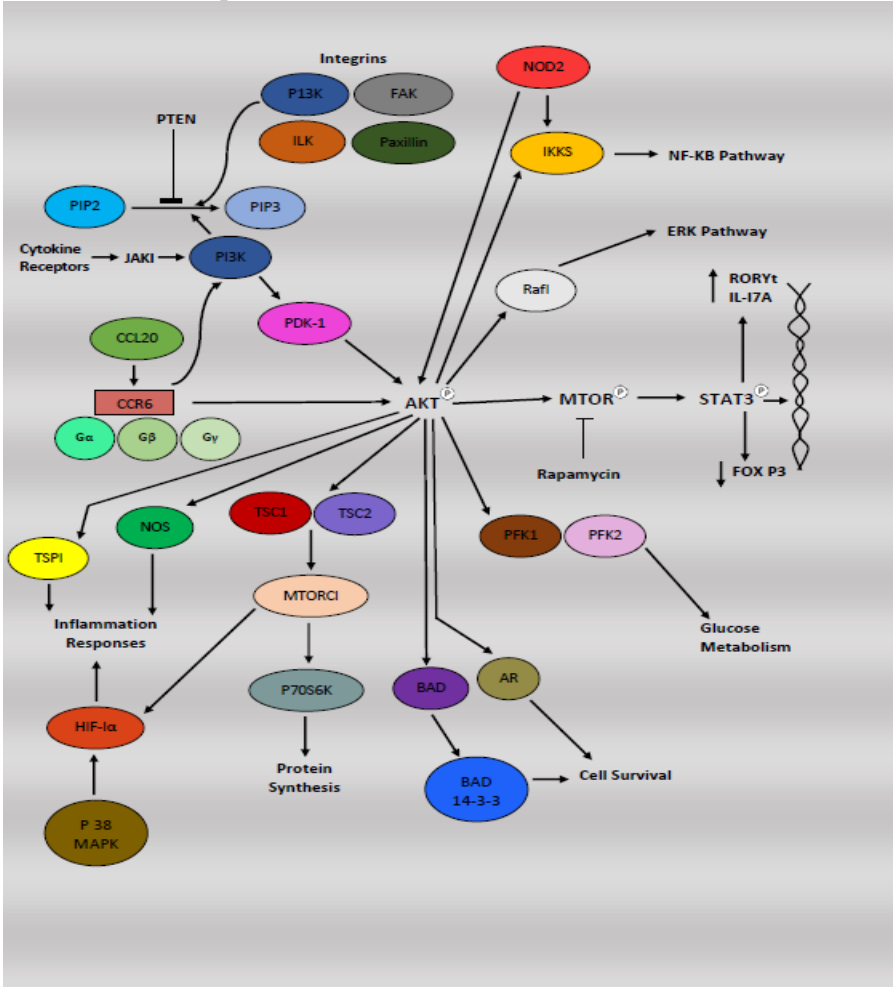

Figure 10: Some possible immune pathways involving PI3K and Akt^{P}.

Legend: Phosphatidylinositol 4,5-bisphosphate (PIP2), Phosphatidylinositol (3,4,5)-trisphosphate (PIP3), Phosphatase and tensin homolog (PTEN), Phosphoinositide 3-kinases (PI3K), 3-Phosphoinositide-dependent protein kinase 1 (PDK1), C-C Chemokine Ligand 20 (CCL20), C-C Chemokine Receptor 6 (CCR6), Guanine nucleotide binding proteins -alpha subunit (Gα), Guanine nucleotide binding protein – beta subunit (Gβ), Guanine nucleotide

binding protein -gamma subunit (Gγ), Thrombospondin-1 (TSP1), Nitric oxide synthase (NOS), Hypoxia-inducible factor 1-alpha (HIF-1α), P38 Mitogen Activated Protein Kinases (p38 MAPK), Tuberous Sclerosis 1 (TSC1), Tuberous Sclerosis 2 (TSC2), Mammalian Target of Rapamycin (mTOR), Mammalian Target of Rapamycin Complex 1 (mTOR C1), Ribosomal Protein S6 Kinase beta - 1 (P70S6K), Phosphofructokinase -1 (PFK-1), Phosphofructokinase-2 (PFK-2), Androgen Receptor (AR), Protein Kinase B (Akt), Phosphorylated Signal Transducer of Activation of Transcription 3 ($STAT3^{P}$), Forkhead Box P3 (FOXP3), RAR-related orphan receptor gamma (t) (RORγt), Interleukin 17 A (IL-17A), **Raf**-1 Proto-Oncogene, Serine/Threonine Kinase (Raf-1), Inhibitor of Kappa B Kinases (IKKS), Nucleotide-binding oligomerization domain-containing protein 2 (NOD2), Focal Adhesion Kinase in Integrin (FAK), Integrin-Linked Kinase (ILK), Janus kinase 1 (JAK-1).

5.0 References

1. Ranasinghe R, Eri R. Modulation of the CCR6-CCL20 Axis: A Potential Therapeutic Target in Inflammation and Cancer. Medicina. 2018;54(5):88.
2. Perera AP, Fernando R, Shinde T, Gundamaraju R, Southam B, Sohal SS, et al. MCC950, a specific small molecule inhibitor of NLRP3 inflammasome attenuates colonic inflammation in spontaneous colitis mice. Scientific reports. 2018;8(1):8618.
3. Robinson AM, Gondalia SV, Karpe AV, Eri R, Beale DJ, Morrison PD, et al. Fecal microbiota and metabolome in a mouse model of spontaneous chronic colitis: Relevance to human inflammatory bowel disease. Inflammatory bowel diseases. 2016;22(12):2767-87.
4. Ng SC, Shi HY, Hamidi N, Underwood FE, Tang W, Benchimol EI, et al. Worldwide incidence and prevalence of inflammatory bowel disease in the 21st century: a systematic review of population-based studies. The Lancet. 2017;390(10114):2769-78.
5. Plevinsky J, Gumidyala A, Fishman L. Transition experience of young adults with inflammatory bowel diseases (IBD): a mixed methods study. Child: care, health and development. 2015;41(5):755-61.
6. Sewitch MJ, Abrahamowicz M, Bitton A, Daly D, Wild GE, Cohen A, et al. Psychological distress, social support, and disease activity in patients with inflammatory bowel disease. The American journal of gastroenterology. 2001;96(5):1470.
7. Hrabe JE, Byrn JC, Button AM, Zamba GK, Kapadia MR, Mezhir JJ. A matched case-control study of IBD-associated colorectal cancer: IBD portends worse outcome. Journal of surgical oncology. 2014;109(2):117-21.
8. Ranasinghe R, Eri R. Pleiotropic immune functions of chemokine receptor 6 in health and disease. Medicines. 2018;5(3):69.
9. Ranasinghe R, Eri R. CCR6–CCL20-Mediated Immunologic Pathways in Inflammatory Bowel Disease. Gastrointestinal Disorders. 2019;1(1):15-29.
10. Basheer W, Kunde D, Eri R. Role of Chemokine Ligand CCL20 and its Receptor CCR6 in Intestinal Inflammation. Immunology and Infectious diseases. 2013;1(2):30-7.
11. Basheer W. Genetic ablation of CCR6 confers differential exacerbation in a spontaneous colitis model: University of Tasmania; 2018.
12. Robinson AM, Rahman AA, Carbone SE, Randall-Demllo S, Filippone R, Bornstein JC, et al. Alterations of colonic function in the Winnie mouse model of spontaneous chronic colitis. American Journal of Physiology-Gastrointestinal and Liver Physiology. 2016;312(1):G85-G102.
13. Heazlewood CK, Cook MC, Eri R, Price GR, Tauro SB, Taupin D, et al. Aberrant mucin assembly in mice causes endoplasmic reticulum stress and spontaneous inflammation resembling ulcerative colitis. PLoS medicine. 2008;5(3):e54.

14. Geboes K, Riddell R, Öst A, Jensfelt B, Persson T, Löfberg R. A reproducible grading scale for histological assessment of inflammation in ulcerative colitis. Gut. 2000;47(3):404-9.
15. Cesta MF. Normal structure, function, and histology of the spleen. Toxicologic pathology. 2006;34(5):455-65.
16. Doucet M, Jayaraman S, Swenson E, Tusing B, Weber KL, Kominsky SL. CCL20/CCR6 signaling regulates bone mass accrual in mice. Journal of Bone and Mineral Research. 2016;31(7):1381-90.
17. Ito T, Carson IV WF, Cavassani KA, Connett JM, Kunkel SL. CCR6 as a mediator of immunity in the lung and gut. Experimental cell research. 2011;317(5):613-9.
18. Ranasinghe R, Eri R. CCR6–CCL20 Axis in IBD: What Have We Learnt in the Last 20 Years? Gastrointestinal Disorders. 2019;1(1):57-74.
19. Blau S, Kohen R, Bass P, Rubinstein A. Relation between colonic inflammation severity and total low-molecular-weight antioxidant profiles in experimental colitis. Digestive diseases and sciences. 2000;45(6):1180-7.
20. Lee A, Eri R, Lyons AB, Grimm M, Korner H. CC chemokine ligand 20 and its cognate receptor CCR6 in mucosal T cell immunology and inflammatory bowel disease: odd couple or axis of evil? Frontiers in immunology. 2013;4:194.
21. Katchar K, Kelly CP, Keates S, O'Brien MJ, Keates AC. MIP-3α neutralizing monoclonal antibody protects against TNBS-induced colonic injury and inflammation in mice. American journal of physiology-gastrointestinal and liver physiology. 2007;292(5):G1263-G71.
22. Kulkarni N, Meitei HT, Sonar SA, Sharma PK, Mujeeb VR, Srivastava S, et al. CCR6 signaling inhibits suppressor function of induced-Treg during gut inflammation. Journal of autoimmunity. 2018;88:121-30.
23. Mateer SW, Cardona J, Marks E, Goggin BJ, Hua S, Keely S. Ex vivo intestinal sacs to assess mucosal permeability in models of gastrointestinal disease. JoVE (Journal of Visualized Experiments). 2016(108):e53250.
24. Turner J-E, Paust H-J, Steinmetz OM, Peters A, Riedel J-H, Erhardt A, et al. CCR6 recruits regulatory T cells and Th17 cells to the kidney in glomerulonephritis. Journal of the American Society of Nephrology. 2010;21(6):974-85.
25. Welsh-Bacic D, Lindenmeyer M, Cohen CD, Draganovici D, Mandelbaum J, Edenhofer I, et al. Expression of the chemokine receptor CCR6 in human renal inflammation. Nephrology dialysis transplantation. 2010;26(4):1211-20.
26. Oo YH, Banz V, Kavanagh D, Liaskou E, Withers DR, Humphreys E, et al. CXCR3-dependent recruitment and CCR6-mediated positioning of Th-17 cells in the inflamed liver. Journal of hepatology. 2012;57(5):1044-51.
27. Arsent'eva N, Semenov A, Lyubimova N, Ostankov YV, Elezo D, Kudryavtsev I, et al. Chemokine receptors CXCR3 and CCR6 and their ligands in the liver and blood of patients with chronic hepatitis C. Bulletin of experimental biology and medicine. 2015;160(2):252-5.
28. Paust H-J, Turner J-E, Riedel J-H, Disteldorf E, Peters A, Schmidt T, et al. Chemokines play a critical role in the cross-regulation of Th1 and Th17 immune responses in murine crescentic glomerulonephritis. Kidney international. 2012;82(1):72-83.
29. Egresi A, Kovács Á, Szilvás Á, Blázovics A. Gut-liver axis in inflammatory bowel disease. A retrospective study. Orvosi hetilap. 2017;158(26):1014-21.
30. Silva J, Brito BS, Silva INdN, Nóbrega VG, da Silva MCS, Gomes HDdN, et al. Frequency of Hepatobiliary Manifestations and Concomitant Liver Disease in Inflammatory Bowel Disease Patients. BioMed research international. 2019;2019.
31. Cyster JG, Schwab SR. Sphingosine-1-phosphate and lymphocyte egress from lymphoid organs. Annual review of immunology. 2012;30:69-94.
32. Ito R, Shin-Ya M, Kishida T, Urano A, Takada R, Sakagami J, et al. Interferon-gamma is causatively involved in experimental inflammatory bowel disease in mice. Clinical & Experimental Immunology. 2006;146(2):330-8.

 doi:10.20944/preprints201912.0238.v1

33. Obermeier F, Kojouharoff G, Hans W, Schölmerich J, Gross V, Falk W. Interferon-gamma (IFN-γ)-and tumour necrosis factor (TNF)-induced nitric oxide as toxic effector molecule in chronic dextran sulphate sodium (DSS)-induced colitis in mice. Clinical and experimental immunology. 1999;116(2):238.
34. Nava P, Koch S, Laukoetter MG, Lee WY, Kolegraff K, Capaldo CT, et al. Interferon-γ regulates intestinal epithelial homeostasis through converging β-catenin signaling pathways. Immunity. 2010;32(3):392-402.
35. Thelemann C, Eren RO, Coutaz M, Brasseit J, Bouzourene H, Rosa M, et al. Interferon-γ induces expression of MHC class II on intestinal epithelial cells and protects mice from colitis. PloS one. 2014;9(1):e86844.
36. Spees AM, Kingsbury DD, Wangdi T, Xavier MN, Tsolis RM, Bäumler AJ. Neutrophils are a source of gamma interferon during acute Salmonella enterica serovar Typhimurium colitis. Infection and immunity. 2014;82(4):1692-7.
37. Sheikh SZ, Matsuoka K, Kobayashi T, Li F, Rubinas T, Plevy SE. Cutting edge: IFN-γ is a negative regulator of IL-23 in murine macrophages and experimental colitis. The Journal of Immunology. 2010;184(8):4069-73.
38. Sands BE, Kaplan GG. The role of TNFα in ulcerative colitis. The Journal of Clinical Pharmacology. 2007;47(8):930-41.
39. Roda G, Marocchi M, Sartini A, Roda E. Cytokine networks in ulcerative colitis. Ulcers. 2011;2011.
40. Maxwell JR, Zhang Y, Brown WA, Smith CL, Byrne FR, Fiorino M, et al. Differential roles for interleukin-23 and interleukin-17 in intestinal immunoregulation. Immunity. 2015;43(4):739-50.
41. Whibley N, Gaffen SL. Gut-busters: IL-17 ain't afraid of no IL-23. Immunity. 2015;43(4):620-2.
42. Huang XL, Xu J, Zhang XH, Qiu BY, Peng L, Zhang M, et al. PI3K/Akt signaling pathway is involved in the pathogenesis of ulcerative colitis. Inflammation research. 2011;60(8):727-34.
43. Setia S, Nehru B, Sanyal SN. Upregulation of MAPK/Erk and PI3K/Akt pathways in ulcerative colitis-associated colon cancer. Biomedicine & Pharmacotherapy. 2014;68(8):1023-9.
44. Yap TA, Garrett MD, Walton MI, Raynaud F, de Bono JS, Workman P. Targeting the PI3K–AKT–mTOR pathway: progress, pitfalls, and promises. Current opinion in pharmacology. 2008;8(4):393-412.

6.0 Acknowledgements

The first author is funded by a research training programme (RTP) scholarship from the Australian government.

7.0 Conflict of Interests

Authors declare no conflict of interests, commercial or financial in writing this article.

8.0 Author Contribution

Conceptualization, Ranmali Ranasinghe; Data curation, Agampodi Promoda Perera, Waheedha Basheer and Paul Scowen; Formal analysis, Ruchira Fernando; Supervision, Madhur Shastri, Terry Pinfold and Rajaraman Eri.